Bond-disordered Anderson model on a two-dimensional square lattice: Chiral symmetry and restoration of one-parameter scaling

Viktor Z. Cerovski
Department of Physics and Astronomy, Michigan State University, East Lansing, Michigan 48824
(Received 28 January 2000; revised manuscript received 21 April 2000)

The bond-disordered Anderson model in two dimensions on a square lattice is studied numerically near the band center by calculating the density of states (DOS), multifractal properties of eigenstates, and the localization length. The DOS divergence at the band center is studied and compared with Gade's result and power law. Although Gade's form describes accurately the DOS of finite-size systems near the band center, it fails to describe the calculated part of the DOS of the infinite system, and a different expression is proposed. Study of the level spacing distributions reveals that the state closest to the band center and the next one have a different level spacing distribution than pairs of states away from the band center. Multifractal properties of finite systems furthermore show that the scaling of eigenstates changes discontinuously near the band center. This unusual behavior suggests the existence of a divergent length scale, whose existence is explained as the finite-size manifestation of the band center critical point of the infinite system, and the critical exponent of the correlation length is calculated by a finite-size scaling. Furthermore, study of the scaling of the Lyapunov exponents of transfer matrices of long stripes indicates that for a long stripe of any width there is an energy region around the band center within which the Lyapunov exponents cannot be described by one-parameter scaling. This region vanishes, however, in the limit of the infinite square lattice, when one-parameter scaling is restored, and the scaling exponent calculated is in agreement with the result of the finite-size scaling analysis.

I. INTRODUCTION

A quantum particle moving in a random potential undergoes the Anderson localization quantum phase transition in three dimensions with increasing strength of disorder.[1–4] The order parameter characterizing the localized phase is the inverse localization length ξ^{-1},[5] describing the exponential decay of the envelope of eigenstates. When the critical point is approached from the localized phase, the localization length, which depends for a given energy only on the strength of the disorder, increases with decreasing disorder strength and finally diverges as a power law at a particular disorder strength. Further decrease of disorder strength then makes the eigenstate extended throughout the whole system. Simultaneously, on length scales smaller than the localization length, eigenstates exhibit multifractal scaling behavior characterized by anomalous scaling of the inverse participation numbers (for definitions and references, see Sec. V).

This basic phenomenon, together with the work of Licciardello and Thouless on the scaling of conductance in finite-size systems,[6] led to the scaling theory of localization,[7,8] one of the main consequences of which is the absence of extended states in two-dimensional disordered systems, with two dimensions being the lower critical dimension of the transition. If spin-orbit interaction is present, however, the picture changes and systems from symplectic ensembles exhibit the localization transition even in two dimensions as opposed to systems from orthogonal ensembles, which have all states localized.[3] The presence of a strong magnetic field in two-dimensional disordered systems, on the other hand, leads to a completely different behavior—the integer quantum Hall effect—where critical states are present at the middle of each of the disorder-broadened Landau levels.[9]

Another class of model exhibiting localization properties different from the systems mentioned above are systems with chiral (particle-hole) symmetry. Such systems are defined on a bipartite lattice with only hopping (off diagonal or bond) disorder. Wegner first realized the importance of this symmetry in disordered systems,[10–12] and even one-dimensional systems with this symmetry are known to have peculiar properties, such as diverging densities of states (DOS's) at the band center,[13] where the eigenstate decays as exp $(-\gamma\sqrt{r})$,[14,15] in contrast to one-dimensional site-disordered systems which have the DOS bounded[16] and all states localized.

There are several models with chiral symmetry that have been extensively studied. The simplest two, in the sense that only one orbital per site and nearest-neighbor hopping are included, time-reversal symmetry is present, and the spin is not relevant, are the Anderson bond-disordered model[13–15,17,18] (ABD) and the random Dirac fermion model (RDF).[19,20] The main difference between these two models is that, in the nondisordered case, the ABD model has a line of points as the Fermi surface at half filling while the RDF model has a point Fermi surface and linear dispersion of energies.

This work is concerned with the ABD model on a square lattice of size L and periodic boundary conditions, defined by the Hamiltonian

$$H = -\epsilon_0 \sum_{\langle i,j \rangle} (t_{i,j} c_i^\dagger c_j + \text{H.c.}), \tag{1}$$

where angular brackets denote neighboring sites on the lattice, c_i is the annihilation operator of the electron at site i, and t's are uniformly distributed random variables $t_{i,j} \in (1-2w,1)$, with $0<w\leqslant 1$. They represent random hopping energies between nearest neighbors, expressed in units of energy ϵ_0, which is set to 1 hereafter.

Interest in this model mainly comes from its unusual scaling properties at the band center, where Soukoulis *et al.*[17] have found a critical state using the Green's function[8] and transfer matrix method (TMM).[21] More recent TMM calculation by Eilmes *et al.*[18] confirmed this result with a higher accuracy and showed the validity of one-parameter scaling not too close to the band center. Nevertheless, Miler and Wang[22] have found in their study of two models with chiral symmetry an apparent band of extended states near the band center, and it remained unclear what is the fate of these states in the infinite two-dimensional (2D) system. Yet another study[23] showed that the scaling exponent of the average participation number changed discontinuously near the band center, and the explicit dependence of this energy on the system size proposed by the authors implied the existence of another diverging length scale in the problem. The last effect is rather subtle to calculate and led to a different participation number scaling exponent of the ABD model at the band center in Ref. 18 compared to the one caluclated here, as discussed in detail in Sec. V below. Furthermore, Brouwer *et al.*[24] have calculated the conductance distribution of quantum wires described by Eq. (1), and showed its nonuniversality and the necessity of introducing an additional microscopic parameter.

It is thus the goal of this paper to present a detailed study of the scaling of the localization length on the approach to the band center for an infinite 2D square lattice, and test the validity of one-parameter scaling, as well as to calculate the multifractal properties of the electron probability density on length scales smaller than the localization length. Also an analytical expression for the DOS of the infinite two-dimensional system near the band center is proposed. This paper is organized as follows. Some general properties and exact results are presented in Sec. II, Calculation of the DOS is presented and analyzed in Sec. III. Section IV contains analysis of level spacing distributions between the nearest neighbors; multifractal properties of eigenstates are studied in Sec. V; scaling of the Lyapunov exponents of transfer matrices of long strips and the scaling of localization length are studied in Sec. VI. Finally, Sec. VII summarizes the results of this work.

II. SOME GENERAL PROPERTIES OF LATTICE HAMILTONIANS WITH CHIRAL SYMMETRY

Suppose that the lattice is composed of two sublattices A and B with, respectively, N_A and N_B sites. The corresponding bond-disordered Hamiltonian with chiral symmetry then has the form

$$H=\sum_{i\in A, j\in B}(t_{i,j}c_i^{\dagger}c_j+\text{H.c.}). \tag{2}$$

It is easy to show that for every eigenstate $|\psi\rangle$ with energy E there is an eigenstate with energy $-E$ with a wave function that has the opposite sign at each site of one of the two sublattices.

If the total number of sites $N=N_A+N_B$ is odd and open bounday conditions are applied (in order to keep the symmetry), then, since all eigenstates come in opposite energy pairs, there will be exactly one state with eigenenergy 0. This can be further generalized, and if $m=N_A-N_B>0$, there exist exactly m zero-energy eigenstates that have vanishing amplitude on the sublattice B.[12,25]

On the other hand, if $m=0$, the electron has equal probability of occupying each of the two sublattices. To show this, Eq. (2) is represented in the basis where the first and second halves of the basis vectors are eigenstates of the position operator on sites of sublattice A and B, respectively. The Hamiltonian is then represented as

$$H=\begin{pmatrix} 0 & M \\ M^{\dagger} & 0 \end{pmatrix}, \tag{3}$$

where M is a square matrix of hopping elements from one sublattice to the other. Eigenstate

$$|\psi\rangle=\begin{pmatrix} |\psi_A\rangle \\ |\psi_B\rangle \end{pmatrix}$$

satisfies

$$E=\langle\psi|H|\psi\rangle=2\,\text{Re}\langle\psi_A|M|\psi_B\rangle. \tag{4}$$

On the other hand,

$$H|\psi\rangle=\begin{pmatrix} M|\psi_B\rangle \\ M^{\dagger}|\psi_A\rangle \end{pmatrix}=\begin{pmatrix} E|\psi_A\rangle \\ E|\psi_B\rangle \end{pmatrix}. \tag{5}$$

From Eqs. (4) and (5) it now follows that, for the ABD model, $\langle\psi_A|\psi_A\rangle=1/2$.

Here only even L finite-size systems on a square lattice with periodic boundary conditions are studied, because one of the main goals of this work is to understand the vicinity of the critical point of the ABD model on the infinite square lattice, which in turn has $m=0$, while the limit $L\to\infty$ for odd L and open boundary conditions has $m=1$.

III. DENSITY OF STATES NEAR THE BAND CENTER

The density of states is calculated by exact numerical diagonalization of finite-size Hamiltonians for various L for many configurations of disorder and binning of eigenenergies. The DOS's obtained for each system size, $\rho_L(E)$, are normalized to 1. The L-dependent parts of such $\rho_L(E)$ are then removed, leaving the L-independent DOS $\rho(E)$, which is therefore expected to be correct in the $L\to\infty$ limit. The removal of finite-size dependency is based on the observation that the DOS converges quickly away from the band center with increasing L. Thus, only a small number of eigenenergies (up to 20) closest to the band center and the corresponding DOS histograms have been calculated for each L. The calculated $\rho_L(E)$ plotted on a single graph revealed that the three bins closest to the band center are where the system size dependence sets in. Their removal thus led to the DOS $\rho(E)$ of the infinite system.

Results for $\rho_L(|E|)$ are given in Fig. 1, for system sizes $L=10,20,\ldots,60$ and number of disordered configurations

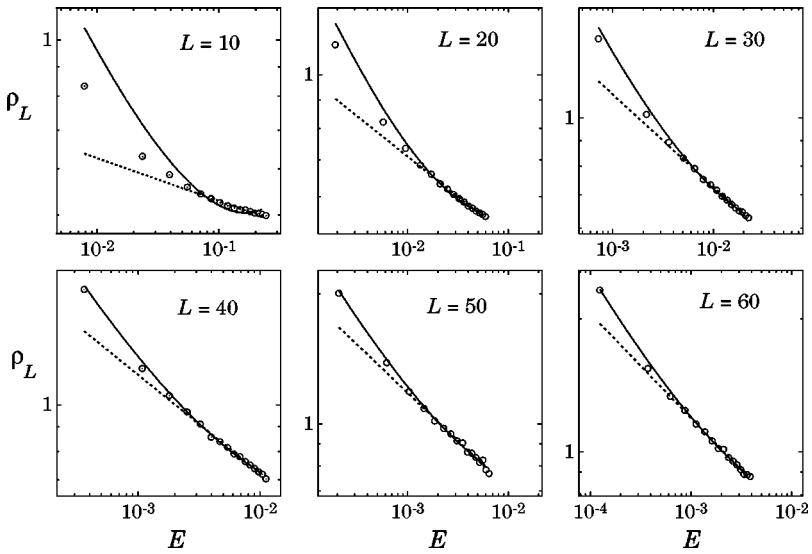

FIG. 1. Density of states $\rho_L(E)$ of the ABD model for $w=1$ near the band center for system sizes $L=10,\ldots,60$ in a log-log plot. Full lines are fits to Gade's form (6), while dotted lines are fits to the power law. The fit to Gade's form is done for all the points except the one closest to the band center, while the fit to the power law is done for all the bins except the three bins closest to the band center, which are the L-dependent parts of $\rho_L(E)$.

ranging, respectively, from 160 000 to 4100. They are fitted to a power law divergence $\rho_L(E)=C_L|E|^{-\alpha_L}$, as well as to Gade's result[11]

$$\rho_L(E)=C_L\frac{1}{|E|}\exp(-\kappa_L\sqrt{-\ln|E|}). \tag{6}$$

All the calculations were done for several different numbers of bins, and the values obtained for the fitting parameters were the same within error bars.

Figure 1 shows that Eq. (6) describes ρ_L very accurately for $L\geqslant 40$, including the size-dependent part. The power law, on the other hand, also describes the data accurately for the same system sizes, but fails to describe the L-dependent part of ρ_L. Despite this, neither of the two forms describes the whole $\rho(E)$ accurately. Instead, the expression found to best fit the L-independent DOS obtained, given in Fig. 2, is

$$\rho(E)=C\frac{1}{\sqrt{|E|}}\exp(-\kappa\sqrt{-\ln|E|}), \tag{7}$$

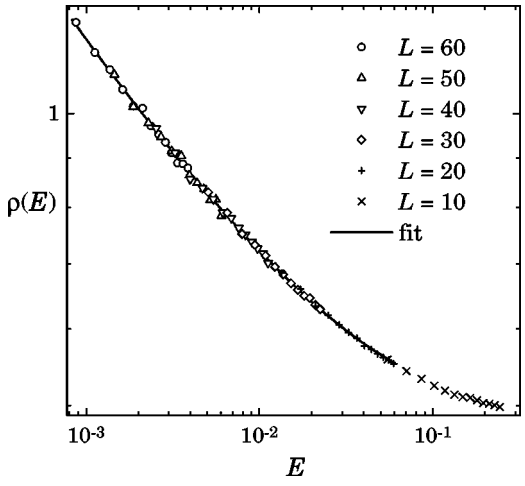

FIG. 2. Density of states of the ABD model for $w=1$ near the band center. The graph is obtained from the data in Fig. 1 by removing the three bins closest to the band center, leaving the L-independent $\rho(E)$. The fit is $\rho(E)=C\exp(-\kappa\sqrt{-\ln|E|})/\sqrt{|E|}$, with $\kappa=1.345\pm0.005$ and $C=1.30\pm0.03$.

with $\kappa=1.345\pm0.005$ and $C=1.30\pm0.03$, represented by the full line in the same figure. The observed range in which Eq. (7) is accurate is for all the energies studied smaller than 6×10^{-2}.

IV. DISTRIBUTION OF THE NEAREST-NEIGHBOR LEVEL SPACINGS

In the localized regime, an eigenstate is determined mainly by a local configuration of disorder where the wave function is localized, and two eigenstates close in energy are spatially far apart. Level repulsion is therefore absent and the distribution of the nearest-neighbor level spacings $s\equiv E_{i+1}-E_i$ is Poissonian,[26]

$$D_P(s)=\frac{1}{\delta}\exp\left(-\frac{s}{\delta}\right), \tag{8}$$

where $\delta\equiv\langle s\rangle$ is the mean level spacing.

In the delocalized phase, on the other hand, eigenstates are extended throughout the system and level repulsion becomes significant for eigenstates with close energies. In the infinite 3D Anderson site-disordered (ASD) model,

$$H=\sum_i \epsilon_i n_i-\sum_{\langle i,j\rangle}(c_i^\dagger c_j+c_j^\dagger c_i), \tag{9}$$

with uniformly distributed $\epsilon_i\in(-W/2,W/2)$, the distribution of level spacings becomes that of the Gaussian orthogonal ensemble,[26] very accurately described by the Wigner surmise

$$D_W(s)=\frac{\pi}{2}\frac{s}{\delta^2}\exp\left[-\frac{\pi}{4}\left(\frac{s}{\delta}\right)^2\right]. \tag{10}$$

In finite-size systems, localized states are on average at a distance L rather than infinitely far apart. This leads to a repulsion between adjacent energy levels and a nonuniversal distribution $D_L(s)$. Shklovskii *et al.*[26] have shown that $D_L(s)$ of the 3D site-disordered Anderson model exhibits a linear dependence on s characteristic for $D_W(s)$ for small s and an exponential tail characteristic for $D_P(s)$ for large s. They were able, from a finite-size scaling analysis of the tail, to accurately determine the critical point and exponent. In

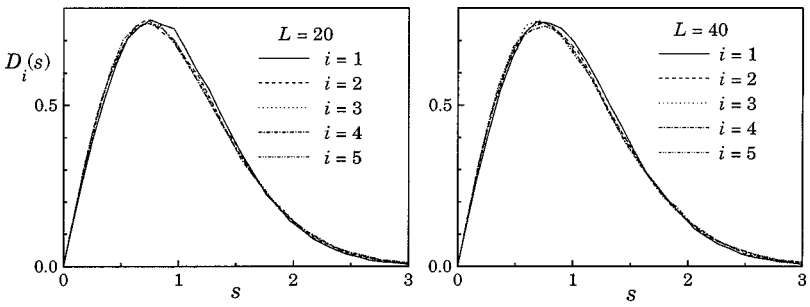

FIG. 3. Distributions of level spacings (after unfolding of the spectrum) $D_i(s)$ between the levels i and $i+1$, counted from the band center. $D_1(s)$ is distinctly different from other distributions due to the presence of symmetry.

the infinite size limit, they recovered not only $D_P(s)$ in the insulating phase and $D_W(s)$ in the conducting phase, but also a system-size-independent nonuniversal distribution at the critical point, which was further shown by Braun *et al.*[27] to be dependent on boundary conditions. This method was also used for an accurate determination of the localization length in the two-dimensional ASD model,[28] confirming the absence of delocalized states following the scenario of the insulating phase from Ref. 26 described above.

To see the effect of the symmetry of the Hamiltonian (2) on the distribution of level spacings, let us for a moment consider the ith eigenenergy E_i of the ASD model. Upon averaging over disorder, the E_i will be distributed between E_i^{min} and E_i^{max} according to some distribution. Some of the eigenenergies, for i close to $N/2$, will have $E_i^{min}<0<E_i^{max}$. This is, however, forbidden for eigenstates of the ABD model since every E_i of Eq. (2) is negative for $i<N/2$ and positive for $i>N/2$. This means that eigenenergies of Eq. (2) close to the band center are effectively pushed away from it due to the symmetry. If L is much smaller than the localization length, states will be repelled among themselves due to their large spatial overlap. But the two states closest to the band center, being simply related to each another by the symmetry, will not repel at all, i.e., the state closest to the band center is at the (high energy) end of the spectrum. Thus, these two states are distributed around zero, where distributions of all other individual levels go to zero.

To explore the consequences of this simple analysis, the level spacing distribution is calculated between each pair of adjacent levels separately. Let us denote by $D_i(s)$ the level spacing distribution between the energy levels i and $i+1$ after unfolding of the spectrum,[29] i.e., expressing level energies in units of the mean level spacing, where $0<E_1<E_2<\cdots<E_{N/2}$. Figure 3 shows $D_1(s),\ldots,D_5(s)$, for $L=20,40$, and, respectively 150 000,120 000 configurations, and it can be seen that $D_1(s)$ is distinctly different from $D_2(s),\ldots,D_5(s)$. The same effect was also present for $L=10,30$, while for $L=50$ and 60 the number of disorder configurations was insufficient for an accurate enough determination of the individual $D_i(s)$.[30] This illustrates how the presence of chiral symmetry can profoundly influence spectral characteristics near the band center, despite the fact that the DOS's of the ABD and ASD models seem to have the same shape for adequately chosen pairs of disorder parameters w and W away from the band center (and after rescaling of ϵ_0).[18]

V. MULTIFRACTALITY OF EIGENSTATES

The eigenstate of an electron in a random potential fluctuates from site to site and it has been proposed that the eigenstate at the mobility edge in disordered systems in general should have a fractal structure,[31] and shown that even localized states in one and two dimensions exhibit fractal character on length scales smaller than the localization length.[32–34]

Inverse participation numbers Z_q (IPN's) are particularly convenient quantities to describe scaling properties of probability distribution of the electron. The IPN's of an eigenstate Ψ are defined as

$$Z_q(\Psi)\equiv\sum_{i=1}^{L\times L}|\Psi(\mathbf{r}_i)|^{2q}. \tag{11}$$

Intuitively, their meaning can be seen by looking at the participation number $Z_2(\Psi)^{-1}$: it is equal to 1 for a state localized at one site and to N for plane waves. The participation number thus gives generally the number of sites at which the wave function is significantly different from zero. The participation numbers $Z_q(\Psi)^{-1}$ generalize this by giving the number of sites where the probability distribution of electrons is very high (for large positive q's), very low (for large negative q's), and in between these extrema is continuously parametrized by q.

More convenient, with the advantage of being defined as averages over disorder at a given energy E, are IPN's defined as functions of E and system size L,

$$Z_q(L,E)\equiv\langle Z_q(\Psi)\,\delta(E(\Psi)-E)\rangle, \tag{12}$$

where the angular brackets denote averaging over disorder. $Z_q(E,L)$ can be numerically calculated by averaging Eq. (11) over all eigenstates from M configurations of disorder belonging to an energy interval of width ΔE around E, and studying the limit $\Delta E\to 0$ for large M.[23]

Wegner[35] pioneered this kind of investigation, and Castellani and Peliti[36] proposed that eigenstates near the critical point are multifractal on length scales smaller than ξ. The most important feature of IPN's of eigenstates is their scaling with system size and energy:[35,36]

$$Z_q(L,E)\sim L^{-\tau_q}, \tag{13}$$

$$Z_q(L,E)\sim|E-E_c|^{\pi_q}, \tag{14}$$

where E_c is the critical energy. The former scaling is present at any E for $L\ll\xi(E)$, while the latter holds in the critical region of the transition.[37]

Within the framework of multifractality,[38,39] the electron probability density is characterized by several quantities that can be derived from τ_q—the generalized dimension D_q and the singularity strength α_q of the qth singularity with the fractal dimension f_q:

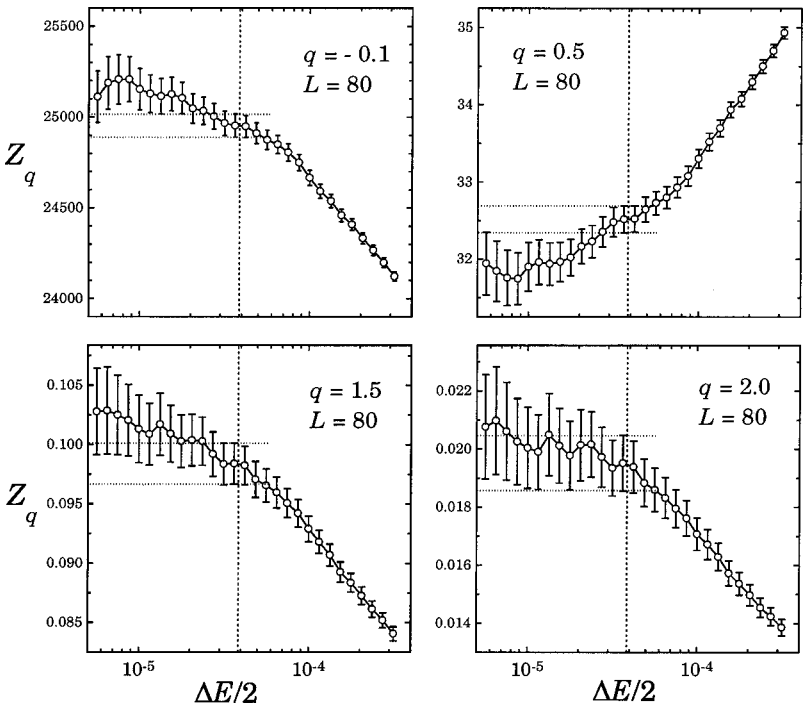

FIG. 4. Dependence of the average IPN for several different q's and $L=80$ on the bin size ΔE. The vertical dashed lines represent energies $E_2(L)/2$ (see text for discussion).

$$(q-1)D_q \equiv \tau_q, \quad \alpha_q \equiv \frac{d\tau_q}{dq}, \quad f_q(\alpha_q) \equiv \alpha_q q - \tau_q. \tag{15}$$

D_q represents a generalization of the fractal dimension, and it is constant and equal to the fractal dimension for ordinary fractals, while $f_q(\alpha_q)$ is the singularity strength spectrum describing a multifractal as an interlaced set of fractals with fractal dimensions f_q, where the measure on the qth fractal scales as a power law with exponent α_q. These quantities have several general properties: D_0 is the fractal dimension of the support (2 in this work); D_1 is called the information dimension since it describes scaling of the entropy of the measure,[40] and there exist finite $D_{min}=D_{q\to\infty}$ and $D_{max}=D_{q\to-\infty}$.

This work is concerned mainly with the spectrum of generalized dimensions D_q characterizing the spatial structure of eigenstates on length scales smaller than the localization length, while the properties of π_q will be discussed elsewhere. Before a detailed discussion of the results, an overview of the main results of this part of the paper is given. The scaling of IPN's at the band center is calculated first, and it is shown that scaling properties (that is, the whole spectrum of generalized dimension D_q) changes discontinuously near the band center, at an energy $E'(L)$ for the range of L studied. It is then shown that E' can be quite accurately identified with half of the width of the energy range around the band center within which two states occur on average in the ensemble of disordered systems. The existence of this energy reveals the existence of a length scale $\xi'(E)$, diverging when $E\to 0$, which is the system size at which the IPN's change their scaling properties from one power law dependence on L to another. This change is then explained as a finite-size manifestation of the critical point, and the critical exponent calculated by a finite-size analysis.

Calculation of $Z_q(E,L)$ starts with calculation of $Z_q(E,L,\Delta E)$, which is just the IPN averaged over all eigenstates from an energy interval $(E-\Delta E/2, E+\Delta E/2)$, taken from N_Ω realizations of disorder, followed by studying the limit $\Delta E\to 0$.[23] Results at the band center for the system $L=80$ and several different q's are presented in Fig. 4. The error bars in the figure are taken to be the standard deviation of the average value.

The figure suggests the existence of an energy E' independent of q (and therefore defined by the whole multifractal measure) such that decreasing ΔE below E' does not change $Z_q(E,L,\Delta E)$ significantly. A decrease of Z_q to a smaller extent, however, is still present for $\Delta E<E'$, and the main source of this is the mismatch between the average and typical values of the IPN at a given energy. Thus, the effect should become smaller as the number of disorder configurations that are averaged over is increased, and $Z_q(E,L,\Delta E<E')\approx Z_q(E,L)$ up to the corresponding statistical error. This can be seen in Figs. 4 and 5, where values of Z_q for $\Delta E<E'$ are approximately constant within the error bars (as indicated by the horizontal dashed lines), while for $\Delta E>E'$ there is approximately a linear dependence of Z_q on the bin size ΔE. In this sense Fig. 5 suggests that E' exists for all the systems studied (and can be shown to be independent of q for each of them, analogously to Fig. 5).

An analogous analysis is carried out for energies away from the band center and $Z_q(E,L)$ determined accordingly, where it turns out that the convergence for these energies is slightly easier to establish and occurs at larger ΔE than at the band center. Such energy intervals used in calculations of IPN's for different E were small enough so that there was essentially no overlap among them.

The vertical dashed lines in Fig. 4 and Fig. 5 represent half of the energy $E_2(L)$, defined as the width of the energy interval around zero in which every system from the ensemble of disordered systems has two states on average,[23]

$$1 = L^2 \int_{E_2/2}^{0} \rho_L(\epsilon)\, d\epsilon. \tag{16}$$

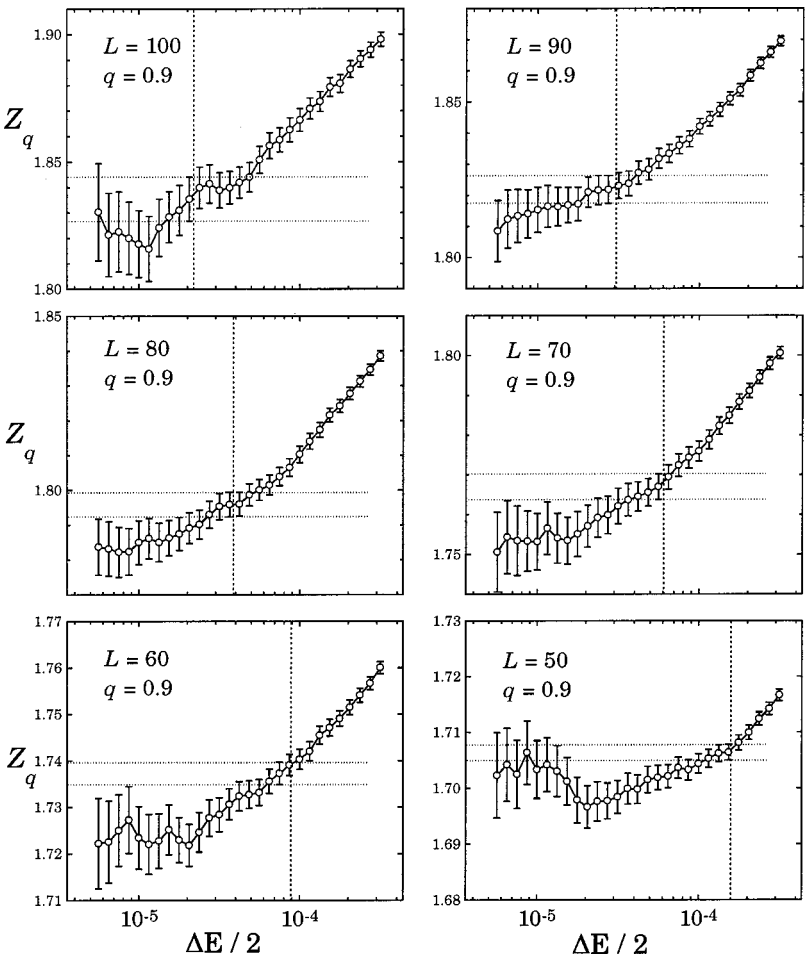

FIG. 5. Dependence of the average IPN for several different L and $q=0.9$ on the bin size ΔE. The vertical dashed lines represent energies $E_2(L)/2$ (see text for discussion).

From the figures one can see that $E' \approx E_2/2$ for all system sizes studied except $L=40$ (the smallest system studied, not shown in Fig. 5), where the convergence seems to be somewhat slower. Equation (16) defines a length scale $\xi'(E)$ that can be described as the system size L for a given energy E such that the number of states within the energy interval between $-E$ and E is 2 on average. This can be defined as

$$\xi'(E) = E_2^{-1}(E), \tag{17}$$

where $E_2^{-1}(E)$ is the inverse function of $E_2(L)$, which is defined by Eq. (16). Since $E_2(L)$ goes to zero when $L \to \infty$, this length scale diverges when $E \to 0$.

It is tempting to integrate results for ρ_L from Sec. III to obtain $\xi'(E)$ explicitly. This, however, does not give the correct result since the whole analysis of the DOS from Sec. III is done for energies larger than the width of the distribution of the two states closest to the band center, which in turn defines ξ' in Eq. (17). In other words, there is an energy cutoff, vanishing when $L \to \infty$, below which the fits are not accurate, most obviously seen by noticing that all of the assumed analytical forms of ρ_L are diverging at the band center, while the actual ρ_L is not.

A nontrivial feature connected with the existence of the length scale ξ' is that the scaling exponents $\tau_q(E)$ are different for $L \lesssim \xi'(E)$ and $L \gtrsim \xi'(E)$. This is a generalization of findings from Ref. 23, where a deviation from the power law scaling of the average participation number for different ΔE at the band center appeared whenever ΔE exceeded $E'(L)$ in several models with chiral symmetry. It can be straightforwardly shown that the same happens with scaling of $Z_q(E=0,L,\Delta E)$. This suggests that a different scaling characteristic should be attributed to the two states closest to the band center, and that E' scales as E_2, with a coefficient of proportionality close to 1. This also implies that the corrections to the constant $Z_q(E,L,\Delta E)$ for $\Delta E < E'$ are small. Therefore, the length at which the change of scaling occurs should be close to and depend on the energy proportionally to $\xi'(E)$, while the change of scaling should be a narrow crossover, as opposed to the much broader crossover from power law to constant IPN that occurs at the termination of the multifractal scaling (13) for $L \approx \xi$.

This is compatible with the results presented in Fig. 6, which gives the calculated $Z_q(L,E)$ for $q=0.9,2$ as well as for all L and E studied. Smaller q's allow for more accurate determination of the scaling properties, and it can be seen from the data that for both q's there are two characteristic scaling behaviors—one occurs at the band center and nearby energies for smaller L, while the other scaling holds at energies further away from the band center, and for larger L at energies close to the band center.

The scaling exponents τ_q are determined from the linear regression of the data for system sizes $L=50,60,\ldots,100$. The goodness of the power law fit is quantitatively characterized by a coefficient $\gamma_q(E)$ next to the quadratic term from an additional quadratic fit of the data. τ_q and γ_q obtained thus from the data in Fig. 6 are presented in Fig. 7.

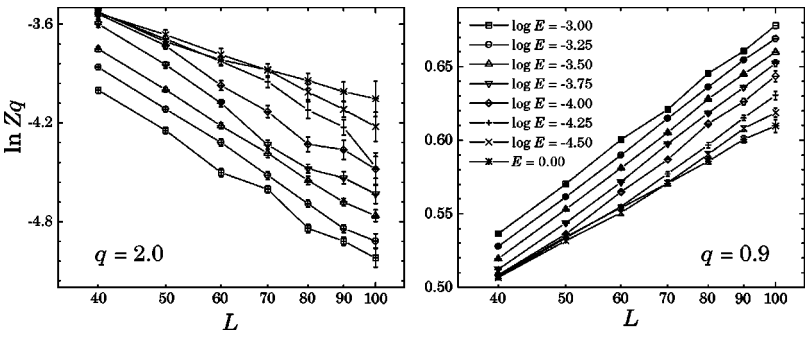

FIG. 6. Dependence of the average IPN on system size for several energies near the band center for $q=0.9,2$.

The results show the existence of three different cases. (i) Away from the band center, $\gamma_q \approx 0$ and τ_q is independent of E, indicating a power law dependence of IPN on L, (ii) Approaching the band center, γ_q becomes different from zero, indicating that a power law is not obeyed. This is due to the emergence of the scaling for system sizes $L \gtrsim \xi'(E)$ discussed above and present in Fig. 6, (iii) For $E=0$ a power law is obeyed again ($\gamma_q \approx 0$), but with a different τ_q than for energies away from the band center.

The discontinuity of $\tau_q(E)$ for all the other q's studied naturally leads to two different spectra of generalized dimensions, and Fig. 8 shows the calculated D_q for all energies except the three nonzero energies closest to the band center (which cannot give τ_q from the fitting procedure used here due to the change of scaling properties discussed above). In particular, the participation number grows with the number of sites L^2 as a power law with exponents $\beta(E=0)=0.25 \pm 0.02$, and $\beta(E\neq 0)=0.55\pm 0.05$. This should be compared with the result for the ABD model of Ref. 18, $\beta(E=0)=0.50\pm 0.06$. It is easy to explain this discrepancy since the bin size $\Delta E=4\times 10^{-4}$ used in Ref. 18 was, depending on the system size, roughly an order of magnitude too large to detect the correct scaling behavior, and therefore $\beta(E\neq 0)$ was obtained instead.

D_q is calculated for only three negative values of q, mainly because IPN's for negative q's are determined mostly by the parts of eigenstates with the smallest probability of finding the electron, which in turn acquire the highest relative error during numerical diagonalization of the Hamiltonian. Difficulties in calculating D_q in this regime even arouse suspicion that multifractality might break down for negative q.[41] It is thus important to show that D_q is defined for negative q's as well as for positive ones. The accuracy of all the calculations of IPN's done in this section can be straightforwardly improved by increasing the number of configurations of disorder that is averaged over. This would lead to smaller error bars of all the quantities calculated, as well as to a wider range of q's for which D_q can be calculated.

The results of this section give the following picture of the scaling of IPN with system size. For any energy E close enough to the band center, there exist two power law scalings: one for $L_0 < L \lesssim \xi'(E)$ described by the set of exponents $\tau_q(E=0)$, and another one for $\xi'(E) \lesssim L \ll \xi(E)$, described by a *different* set of exponents $\tau_q(E\neq 0)$, which leads to the two different spectra of generalized dimension D_q.

The dependence of the additional length scale on energy, $\xi'(E)$, can easily be determined from Eq. (17) by integrating the actual numerical data for $\rho_L(E)$, and the result, obtained from Fig. 9, gives $\xi'(E) \propto |E|^{-\nu'}$, with

$$\nu' = 0.35 \pm 0.01. \tag{18}$$

The meaning of this length scale and corresponding exponent ν' can be understood by assuming that the additional scaling of the two states is due to the finite-size effect of ''smearing'' of the $E=0$ critical point of the infinite system, because exactly the two states closest to the band center become critical when $L\to\infty$. The critical energy then changes by $\Delta\epsilon$ which is, in a finite system of size L (in units of the

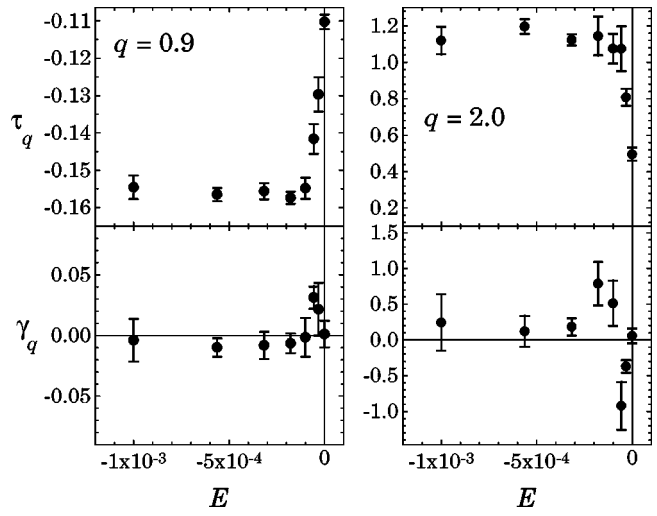

FIG. 7. Scaling exponent of IPN, τ_q, and the goodness of fit coefficient γ_q, calculated from the data in Fig. 6 (except $L=40$ results).

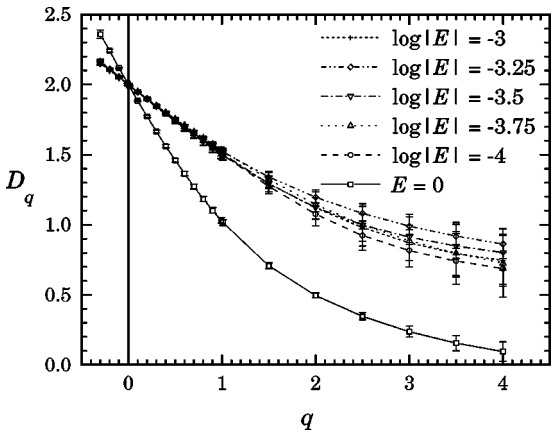

FIG. 8. Multifractal spectra D_q at the band center and nearby energies.

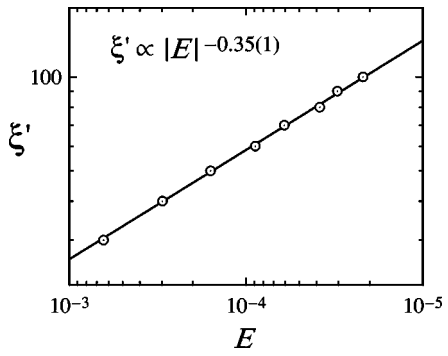

FIG. 9. Dependence of the additional length scale on energy near the band center, as determined from Eq. (17).

lattice spacing), equal to $\Delta E_2(L) \propto L^{-\delta} = L^{-1/\nu'}$. If, furthermore, $\xi \propto |E|^{-\nu}$ in the infinite system, the shift $\Delta\epsilon_c$ of the critical energy in the system of size L is $\Delta\epsilon_c \propto L^{-1/\nu}$, from the general theory of finite-size scaling.[42] Therefore, ν' equals ν, the critical exponent of the correlation length of the infinite two-dimensional system. It should be noted that the finite-size scaling applied here is somewhat different from usual, where $\Delta\epsilon_c \equiv |E-E_c|/E_c$.[42] Here, $E_c = 0$ and $\Delta\epsilon_c \equiv |E-E_c|$, where both energies are expressed in units of ϵ_0, as discussed in the Introduction. Thus, the energy ϵ_0 appears in the denominator of $\Delta\epsilon_c$ rather than the critical energy itself.

VI. LOCALIZATION LENGTH NEAR THE BAND CENTER

In order to calculate the localization length of the infinite two-dimensional system, the finite-size scaling (FSS) analysis of MacKinnon and Kramer[8] is applied to the TMM of Pichard and Sarma.[21] In this analysis, renormalized inverse Lyapunov exponents (ILE's) of the transfer matrix of the ABD model[18,24] of a long quasi-one-dimensional strip of width M are calculated for several energies near the band center and one parameter scaling analysis is applied to the largest ILE, from which the correlation length of the 2D system is calculated. The scaling analysis consists of assuming that the change of the largest ILE, $\Lambda(E,M)$, due to rescaling $M \to bM$ can be compensated by an appropriate change of energy, after which Λ will remain the same, which implies that[8]

$$\Lambda(E,M) = \Lambda(M/\xi(E)). \tag{19}$$

Figure 10 shows the calculated $\Lambda(E,M)$ for several energies E close to the band center and for various strips up to 128 sites wide. The figure also gives the second largest (dashed line) renormalized ILE, Λ_2, for the two lowest nonzero energies studied ($E = 10^{-5}$ and 10^{-6}) and for $M \leqslant 20$. All values are obtained with relative error of 1% or better.

At $E = 0$ and for M even, all ILE's become doubly degenerate due to the presence of chiral symmetry,[22,24] and they scale linearly with M for $M \geqslant 16$, reflecting the scale invariance of Λ characteristic of a critical state. To see the effect this degeneracy has on the scaling properties of ILE's, we should recall that ILE's of transfer matrices of disordered systems repel each other in general[43] and become self-averaging quantities for sufficiently long stripes.[21] The symmetry now enforces ''dimerization'' of pairs of ILE's, acting as an effective attractive force between each pair of ILE's that becomes degenerate at zero energy, as in Fig. 10, where, for a fixed M, Λ, and Λ_2 are closer together for smaller energy. The largest ILE thus decreases in a strip of width M on approaching the band center, as in models with chiral symmetry studied in Ref. 22. On the other hand, at any given energy, every pair of ILE's becomes more repulsive with increasing M. Such an increased number of ILE's thus diminishes the attractive effect of the symmetry, and, depending on the relative strengths of the two effects, there are two regimes: (i) for smaller M, the largest ILE increases approximately linearly with M, and, since the slope of the rise changes with energy, FSS cannot be done; (ii) for sufficiently large M, on the other hand, the repulsion among ILE's due to disorder dominates and FSS is possible.

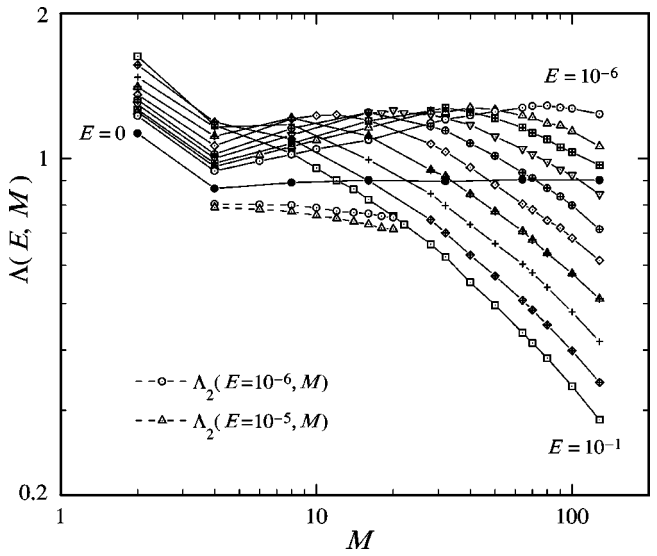

FIG. 10. The largest renormalized inverse Lyapunov exponents $\Lambda(E,M)$, calculated for long stripes of width M and various energies near the band center (full line). The energy range is $\log_{10}|E| = -1, -1.5, \ldots, -5, -6$. Dashed lines connect points of the second largest ILE, $\Lambda_2(E,M)$, for energies $E = 10^{-5}, 10^{-6}$, and $M \leqslant 20$.

The one-parameter universal function $\Lambda(M/\xi(E))$, obtained for system sizes $M \geqslant 50$ for energies $|E| > 10^{-4}$, and for system sizes $M \geqslant 64$ for energies $10^{-5} \leqslant |E| \leqslant 10^{-4}$, is presented in Fig. 11. The obtained localization length $\xi(E)$, in units of the localization length of the smallest energy studied ($E = 0.1$), is shown in the inset of the same figure. The calculated $\xi(E)/\xi(0.1)$ is fitted to a power law for energies $10^{-5} \leqslant E \leqslant 10^{-3}$, and the result suggests a power law diverging localization length at the band center, with the exponent

$$\nu = 0.335 \pm 0.034, \tag{20}$$

in agreement with the result (18) of Sec. V.

Some additional analysis of the results can be done by introducing $\Lambda_{max}(M)$, defined as the maximal $\Lambda(E,M)$ for a given strip width M. The importance of this quantity comes from the fact that points where Λ reaches its maximum for various energies cannot be described by FSS, and, at the same time, Λ_{max} limits by its definition possible values that $\Lambda(x)$ (obtained from the FSS) can have. The main observa-

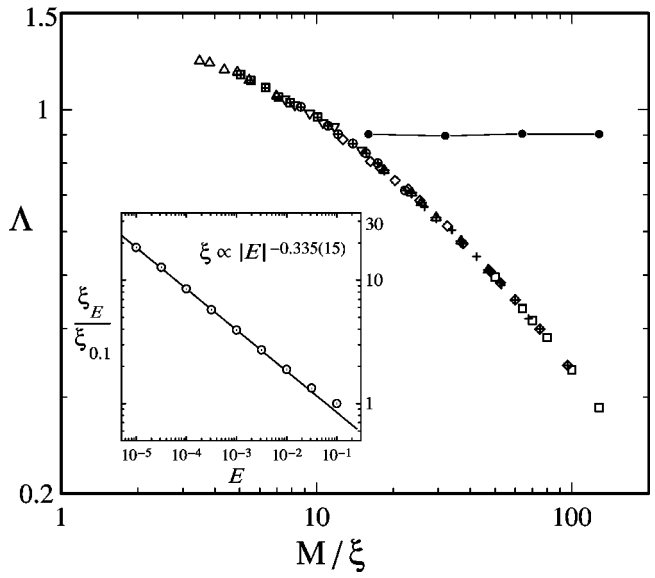

FIG. 11. One-parameter universal function $\Lambda(M/\xi(E))$ for the ABD model. The four separate points are $\Lambda(E=0,M)$ for $M=16,32,64,128$, corresponding to the band center critical state. The inset shows the calculated localization length $\xi(E)$ in units of the localization length $\xi(E=0.1)$, with error bars smaller than the symbol size.

tion is that Λ_{max} seems to grow slower than linearly in Fig. 10. Linear (or faster) growth would imply the existence of an additional energy scale below which FSS would break down for all large M and $\Lambda(E,M)$ would grow linearly and indefinitely with M in the same figure, implying the existence of a whole band of extended states where one-parameter scaling would not hold. The slower than linear growth of Λ_{max} seen, therefore, further suggests the existence of a single critical point at the band center of the system on an infinite square lattice.

VII. CONCLUSIONS

In conclusion, the main results of this work are summarized. The densities of states of finite-size systems are calculated and the validity of Gade's expression (6) is shown. The calculated part of the DOS for the system on an infinite square lattice, however, suggests a different dependence on energy near the band center,

$$\rho(E)=C\frac{1}{\sqrt{|E|}}\exp(-\kappa\sqrt{-\ln|E|}), \tag{21}$$

with $\kappa=1.345\pm0.005$ and $C=1.30\pm0.03$.

Other calculated quantities share in common the qualitative feature of a discontinuous change near or at the band center. The nearest-neighbor level spacing distributions, for instance, between the state closest to the band center and the next one seem to be distinctly different from the level spacing distributions between other neighboring states. This was argued to be connected to the chiral symmetry of the model, which places the two states closest to $E=0$ at the (high energy) end of the spectrum. These two states are further found to play a crucial role in explaining the discontinuous change of the scaling properties of IPN's near the band center. Extrapolation to the limit of the infinite square lattice then led to two different spectra of generalized dimension D_q—one for $E\neq0$ (present at length scales smaller than the localization length), and another one for $E=0$ (present at all length scales). Finite-size scaling associated with the effects that finite L has on the critical band center states of the infinite system led to the value $\nu=0.35\pm0.01$ of the critical exponent of the localization length.

Additional scaling analysis of ILE's of transfer matrices of long quasi-1D systems gave the value $\nu=0.335\pm0.034$. This suggests that there is only one critical state at the band center with all other states localized in the system on the infinite square lattice, in agreement with the findings of Refs. 32 and 18. A one-parameter universal function $\Lambda(x)$ is calculated and another discontinuity found, since $\Lambda(x(E\rightarrow0))\neq\Lambda(E=0,M)$.

A puzzling feature of the critical exponent ν of the ABD as well as of the RDF model[19,20] is their apparent disagreement with the rigorous theorem of Chayes *et al.*,[44] which states that $\nu\geqslant1$ in two-dimensional quantum disordered systems in general. This question, however, requires further study and will be addressed elsewhere.

ACKNOWLEDGMENTS

This work was partially supported by the Department of Physics and Astronomy at Michigan State University. The author is thankful to S. D. Mahanti for suggestions on improving the manuscript and to S. A. Trugman, R. Bhatt, T. A. Kaplan, V. Zelevinski, M. Mostovoy, I. Herbut, D. Mulhall, B. Nikolić, and M. Milenković for inspiring discussions.

[1] P.W. Anderson, Phys. Rev. **109**, 1492 (1958).
[2] D.J. Thouless, Phys. Lett., C **13**, 93 (1970).
[3] P.A. Lee and T.V. Ramakrishnan, Rev. Mod. Phys. **57**, 287 (1985).
[4] B. Kramer and A. MacKinnon, Rep. Prog. Phys. **56**, 1469 (1993).
[5] P.W. Anderson, D.J. Thouless, E. Abrahams, and D.S. Fisher, Phys. Rev. B **22**, 3519 (1980).
[6] D.C. Licciardello and D.J. Thouless, Phys. Rev. Lett. **35**, 1475 (1975).
[7] E. Abrahams, P.W. Anderson, D.C. Licciardello, and T.V. Ramakrishnan, Phys. Rev. B **42**, 673 (1979).
[8] A. MacKinnon and B. Kramer, Phys. Rev. Lett. **47**, 1546 (1981); Z. Phys. B: Condens. Matter **53**, 1 (1983).
[9] B. Huckestein, Rev. Mod. Phys. **67**, 357 (1995).
[10] F. Wegner, Phys. Rev. B **19**, 783 (1979).
[11] R. Gade, Nucl. Phys. B **398**, 499 (1993).
[12] M. Inui, S.A. Trugman, and E. Abrahams, Phys. Rev. B **49**, 3190 (1994).

[13] G. Theodeorou and M. Cohen, Phys. Rev. B **13**, 4597 (1976).
[14] L. Fleishman and D.C. Licciardello, J. Phys. C **10**, L125 (1977).
[15] C.M. Soukoulis and E.N. Economou, Phys. Rev. B **24**, 5698 (1981).
[16] F. Wegner, Z. Phys. B: Condens. Matter **44**, 9 (1981).
[17] C.M. Soukoulis, I. Webman, G.S. Grest, and E.N. Economou, Phys. Rev. B **26**, 1838 (1982).
[18] A. Eilmes, R.A. Römer, and M. Schreiber, Eur. Phys. J. B **1**, 29 (1998).
[19] Y. Hatsugai, X.-G. Wen, M. Kohmoto, Phys. Rev. B **56**, 1061 (1997).
[20] Y. Morita and Y. Hatsugai, Phys. Rev. Lett. **79**, 3728 (1997); Phys. Rev. B **58**, 6680 (1998).
[21] J.L. Pichard and G. Sarma, J. Phys. C **14**, L127 (1981); **14**, L617 (1981).
[22] J. Miler and J. Wang, Phys. Rev. Lett. **76**, 1461 (1996).
[23] V.Z. Cerovski, S.D. Mahanti, T.A. Kaplan, and A. Taraphder, Phys. Rev. B **59**, 13 977 (1999).
[24] P.W. Brouwer, C. Mudry, and A. Furusaki, Nucl. Phys. B **565**, 653 (2000).
[25] It is assumed here, without loss of generality, that $N_A \geqslant N_B$. The *m* zero-energy eigenstates still remain if arbitrary hoppings are introduced among sites of the sublattice *B* (Ref. 12).
[26] B.I. Shklovskii, B. Shapiro, B.R. Sears, P. Lambrianides, and H.B. Shore, Phys. Rev. B **47**, 11 487 (1993). See also E. Hofstetter and M. Schreiber, *ibid.* **48**, 16 979 (1993); Phys. Rev. Lett. **73**, 3137 (1994).
[27] D. Braun, G. Montambaux, and M. Pascaud, Phys. Rev. Lett. **81**, 1062 (1998).
[28] I.Kh. Zarekeshev, M. Batsch, and B. Kramer, Europhys. Lett. **34**, 587 (1996).
[29] F. Haake, *Quantum Signatures of Chaos* (Springer-Verlag, Berlin, 1991). Unfolding by the cubic spline fitting was used.
[30] Some preliminary results indicate that $D_1(s)$ has characteristics of the critical distribution, while other $D_i(s)$ have the exponential tail characteristic for localized states.
[31] H. Aoki, J. Phys. C **16**, L205 (1983); Phys. Rev. B **33**, 7310 (1986).
[32] C.M. Soukoulis and E.N. Economou, Phys. Rev. Lett. **52**, 565 (1984).
[33] M. Schreiber, J. Phys. C **18**, 2493 (1985); Phys. Rev. B **31**, 6146 (1985).
[34] V.I. Fal'ko and K.B. Efetov, Europhys. Lett. **32**, 627 (1995); Phys. Rev. B **52**, 17 413 (1995).
[35] F. Wegner, Z. Phys. B: Condens. Matter **36**, 209 (1980).
[36] C. Castellani and L. Peliti, J. Phys. A **19**, L429 (1986).
[37] One may imagine that, in the spirit of renormalization group analysis, weaker than power law behavior should be possible as well. This indeed happens with two-dimensional random Dirac fermions interacting with a disordered non-Abelian vector potential, as shown by J.-S. Caux, N. Taniguchi, and A.M. Tsvelik, Phys. Rev. Lett. **80**, 1276 (1998).
[38] T. Hasley, M. Jensen, L. Kadanoff, I. Procaccia, and B. Shraiman, Phys. Rev. A **33**, 1141 (1986).
[39] M.H. Jensen, L.P. Kadanoff, and I. Procaccia, Phys. Rev. A **36**, 1409 (1987).
[40] $D_{q=1}$ is defined from the limit $q \rightarrow 1$ of the definition (15). See, e.g., Ref. 9.
[41] S.N. Evangelou, Physica A **167**, 199 (1990).
[42] J. Cardy, *Scaling and Renormalization in Statistical Physics* (Cambridge University Press, Cambridge, 1996).
[43] C.W.J. Beenakker, Rev. Mod. Phys. **69**, 731 (1997).
[44] J.T. Chayes, L. Chayes, D.S. Fisher, and T. Spencer, Phys. Rev. Lett. **24**, 2999 (1986).